

## **UC Davis**

### **UC Davis Previously Published Works**

#### **Title**

Cellulose nanocrystals and self-assembled nanostructures from cotton, rice straw and grape skin: a source perspective

#### **Permalink**

<https://escholarship.org/uc/item/74n7f8fn>

#### **Journal**

Journal of Materials Science, 48(22)

#### **ISSN**

0022-2461

#### **Author**

Hsieh, You-Lo

#### **Publication Date**

2013-11-01

#### **DOI**

10.1007/s10853-013-7512-5

Peer reviewed

## Cellulose nanocrystals and self-assembled nanostructures from cotton, rice straw and grape skin: a source perspective

You-Lo Hsieh

Received: 15 March 2013 / Accepted: 5 June 2013 / Published online: 20 June 2013  
© Springer Science+Business Media New York 2013

**Abstract** Cellulose nanocrystals (CNCs) have been derived by sulfuric acid hydrolysis (64–65 wt%  $\text{H}_2\text{SO}_4$ , 10 mL/g cellulose, 45 °C) of pure cellulose isolated from cotton, rice straw and grape skin, producing relatively consistent products in 60, 45 and 30 min, respectively, and generally reflecting the extent of crystallinity and crystallite sizes of these cellulose sources. CNCs in nanorod forms are observed from all three cellulose sources and, in the case of cotton and grape skin, in the presence of more dominant forms of nanoparticles. Cotton CNCs are <10-nm-wide nanorods at up to 40 aspect ratios, whereas rice straw CNCs are flat ribbon cross-sectional shaped in 10:2:1–44:5:1 length/width/thickness ratios, and those from grape skin are abundant nanoparticles but fewer nanorods, all of very different nanoscale dimensions. Freezing (–196 °C) and freeze-drying (–50 °C) of dilute CNC suspensions induce self-assembling of these CNC populations into yet further distinctly different morphologies. Self-assembled cotton CNCs are loosely organized nanorods and nanospheres, whereas grape skin CNCs are mainly nanospheres of 5-nm-sized nanoparticles clusters around nanorod cores. Uniquely, rice straw CNCs assembled anisotropically into ultra-thin non-porous fibers. These source-linked unique CNC geometries and the ability of CNCs to self-assemble into different morphologies present wide ranging dimensions of these renewable cellulose

nanomaterial building blocks from by-products of the world largest fiber, cereal and fruit crops.

Cellulose, nature's most abundant polymer, is synthesized by plants as well as some microbes and marine animals. Cellulose is the most chemically homogeneous biopolymer, i.e., a linear syndiotactic homopolymer of  $\beta$ -(1 → 4)-glycosidic bonds linked D-anhydroglucopyranose that contains three hydroxyl –OH groups: one primary –OH on C6 and two secondary –OH on C2 and C3. The lack of free rotation of the C–O–C link gives the steric-specific chain conformation and rigidity that is further reenforced by the extensive inter-molecular and intra-molecular hydrogen bonds to give highly crystalline fibrillar structure in cellulose. As a major cell wall component, cellulose fibrils play a significant role in contributing to strength [1].

Native cellulose consists of hierarchical fibrillar structure. By removing the less ordered cellulose, crystalline nanofibrils have been extracted from a broad range of sources including algae [2], tunicate [3], bacteria [4] and wood [5]. The nanoscale dimensions of these cellulose fibrils are mostly 5–20 nm wide and 100–400 nm long and have been found to vary by method of isolation. Some of the highest aspect ratios reported ranged from 40 for cotton (~200 nm long and 5 nm wide) [6] to over 60 for tunicin whiskers (~1  $\mu\text{m}$  long and 15 nm wide) [7]. These crystalline cellulose nanorods have been commonly referred to as cellulose nanocrystals (CNCs) in the USA and cellulose nanowhiskers in Europe and elsewhere.

Cellulose nanocrystals are best known for their ultra-high strength and low thermal expansion coefficient in the axial direction in addition to their unique nanoscale width dimensions. The bending strength and modulus of CNCs have been estimated [8–10] and measured by Raman

---

**Electronic supplementary material** The online version of this article (doi:10.1007/s10853-013-7512-5) contains supplementary material, which is available to authorized users.

---

Y.-L. Hsieh (✉)  
Fiber and Polymer Science, University of California, Davis,  
Davis, CA 95616, USA  
e-mail: ylhsieh@ucdavis.edu

spectroscopy [10] to be impressively high at  $\sim 10$  and  $\sim 150$  GPa, respectively. This bending strength makes CNCs stronger than the strongest synthetic polyaramids (e.g., Kevlar), glass and steel and approaching one-sixth of the 63 GPa of carbon nanotubes (CNTs) whose tensile strength is predicted to be as high as  $\sim 300$  GPa at a impressive modulus of  $\sim 1$  TPa [11, 12].

Nanocellulose has been derived from a wide range of sources; however, most studies of nanocellulose have evolved from commercially available microcrystalline cellulose (MCC) derived from wood pulp [13]. Nanocellulose derived from feedstock of low- or no-value sources such as agriculture crop and processing industry by-products has been less reported. As cell wall structure and chemical compositions differ among plants, the cellulose molecular chain lengths and fibrillar morphologies also vary. However, studies to date tend to report only the rod-like and/or fibril-like nanocellulose. It is of fundamental scientific interest to gain an understanding of how nanocellulose structures and properties may vary among different plant sources from which they are derived. It is also of great resource and environmental interest to derive potentially high-value nanocellulose from low value and underutilized agricultural and processing by-products.

This paper presents the analyses of cellulose nanocrystals produced by sulfuric acid hydrolysis of cellulose derived from three sources, i.e., cotton, rice straw and grape skins, to give a source perspective. These crops are globally significant, as cotton, rice and grape are the world largest fiber, cereal and fruit crops, respectively [14]. As the purest form of cellulose, cotton fibers are excellent fiber of choice for textiles and as absorbents as is. Rice straw and grape skins, on the other hand, are underutilized crop and beverage processing by-products. This work, therefore, highlights the source link aspect of nanocellulose and gains better understanding on structural transformation during freezing and freeze-drying. Both are important for developing potential use for these renewable resources while also reducing environmental impact of our food supply chain.

Cotton is unique in many ways. Cotton fibers are nearly 90 % cellulose [15], consisting the highest cellulose content among plant cells. The secondary cell wall of cotton is 100 % pure cellulose, making deriving pure cellulose relatively easy once the very thin primary cell wall is removed. Cotton cellulose also has the longest molecular chain lengths as well as the most crystalline structure. Therefore, cotton is an example of an utmost orderly cellulose structure. Rice straw has been reported to contain 32–47 % cellulose, 19–27 % hemicellulose and 5–24 % lignin [16]. The cellulose content in rice straw is therefore close to wood, but far less than cotton or other bast fibers such as flax or jute that consist about 70 % cellulose. Yet,

red grape skins have been reported to contain only 20.8 % cellulose (CrI 66.1 %), although grape stalks have been reported to have more cellulose at 30–38 % [17, 18]. In addition to their lower cellulose contents, rice straw and grape skin cellulose is imbedded within matrices of various polysaccharides, lignins and others, thus requiring multi-step extraction.

A streamlined three-step  $\text{NaClO}_2/\text{KOH}$  process has been established to remove wax, lignin and hemicellulose from rice straw, yielding at least 37 % pure cellulose [19]. Pure cellulose was isolated from Chardonnay grape skins by organic extraction, acid and base dissolutions, and basic and acidic oxidation to yield 16.4 % cellulose [20]. Pure cellulose from cotton, rice straw and grape skins was hydrolyzed with sulfuric acid (64–65 %  $\text{H}_2\text{SO}_4$  45 °C) to cellulose nanocrystals (CNCs). The CNC dimensions and freeze-drying induced morphology and crystalline structures were further analyzed and compared with respect to their sources.

## Experimental

Cotton cellulose used was already purified filter paper (Q2, Whatman). Pure rice straw cellulose was obtained by extracting with 2:1 toluene/ethanol to remove waxes, then treated with 1 % NaOH at 55 °C for 2 h to remove hemicellulose and silica, and finally immersed in 1 %  $\text{H}_2\text{O}_2$  at 45 °C for 6 h to remove lignin. Chardonnay grape skin cellulose was isolated by extracting with 2:1 v/v toluene/ethanol to remove wax, phenolics, pigments and oils, followed by immersion in 2 %  $\text{H}_2\text{SO}_4$  at 90 °C for 5 h to hydrolyze acid soluble polysaccharides and polyphenolics, then leached with 5 % NaOH at 90 °C for 5 h to dissolve hemicellulose and other base soluble polysaccharides, and finally bleached by 5 %  $\text{H}_2\text{O}_2$  at alternating pH 11.5 (45 °C, 8 h) and pH 3–4 (70 °C, 5 h) to remove all remaining impurities. Sulfuric acid (95–98 %) for hydrolysis was provided by EMD. Water used in all experiments was purified by a Millipore Milli-Q UF Plus water purification system.

All pure cellulose was milled to pass through a 60-mesh screen and then hydrolyzed in 64–65 wt% sulfuric acid (10 mL/g cellulose) at 45 °C for 15–60 min. Hydrolysis was stopped by diluting with 10-fold cold (4 °C) water. The suspension was washed once by centrifugation at 4500 rpm for 10 min and then dialyzed with regenerated cellulose dialysis membranes with 12–14 kDa molecular weight cutoff and against ultra-pure water until neutral. The suspension was sonicated (Branson ultrasonic processor model 2510) in an ice bath for 2 h, 30 min and 30 min for cotton, rice straw and grape CNCs, respectively. The suspension was kept over ion-exchange resin for

7 days and filtered. The final concentrations were ca. 0.75, 0.06 and 0.01 wt/wt% for cotton, rice straw and grape skin CNCs, respectively. To dry CNC into solids, each dilute CNC suspension was quickly frozen by pouring liquid nitrogen into the sample container and freeze-dried overnight.

The CNCs derived by acid hydrolysis were characterized from suspensions as well as after freeze-dried. The specific procedures have been previously reported [6, 19, 21] and are briefly described as follows. The CNCs in suspensions were characterized by transmission electron microscopy (TEM, Philip CM12 transmission electron microscope) and atomic force microscopy (AFM, Asylum-Research MFP-3D). The freeze-dried samples were characterized by scanning electron microscope (SEM, XL 30-SFEG, FEI/Philips, USA). For TEM observation, a drop of 10  $\mu$ L diluted CNC suspension (0.001 w/w%) was deposited onto glow-discharged carbon-coated TEM grids (300-mesh copper, formvar-carbon, Ted Pella, Inc., Redding, CA) and the excess liquid was removed by blotting with a filter paper. The specimens were then negatively stained with 2 % uranyl acetate solution for 2 min, blotted with a filter paper to remove excess stain solution and allowed to dry at ambient condition. For AFM, a few drops of CNC suspension (0.001 w/w%) were deposited onto a freshly cleaved mica surface (Highest Grade V1 Mica Discs, 15 mm, Ted Pella, Inc.) and allowed to dry. Samples were scanned at ambient relative humidity and temperature in tapping mode with OMCL-AC160TS standard silicon probes (tip radius <10 nm, spring constant = 28.98 N/m, resonant frequency =  $\sim$ 310 kHz) (Olympus Corp.) under a 1 Hz scan rate and an image resolution of 512  $\times$  512 pixels. Image processing was performed with Igor Pro 6.21 loaded with MFP3D 090909 + 1409 modulus. The diameters and heights were determined from AFM height images. For SEM, samples were mounted on aluminum stubs with conductive carbon tapes and sputtered with gold under vacuum at 20 mA for 2 min (Bio-Rad SEM coating system). The samples were observed and imaged at a 5-mm working distance and a 10-kV accelerating voltage.

## Results and discussion

### Isolation of cellulose

Pure cellulose derived from cotton, rice straw and Chardonnay grape skins is generally fibrillar in irregular tens of micrometers or larger sized structures (Fig. 1). Cotton cellulose retains some resemblance of single-cell fiber form, while grape skin cellulose is the most irregular and least fibrillar. The gross morphologies of the pure cellulose isolated from rice straw and grape skin are similar to

cellulose isolated from other biomass. As the non-cellulosic components are removed by dissolution, cellulose fibrils associate with each other by forming new hydrogen bonds in the drying process.

### Cellulose nanocrystals by sulfuric acid hydrolysis

Pure cellulose was sulfuric acid hydrolyzed (8.75 mL/g, 65 % H<sub>2</sub>SO<sub>4</sub>, 45 °C) into cellulose nanocrystals (CNCs). The lengths of hydrolysis time were 60, 30–45 and 30 min for cotton, rice straw and grape cellulose, respectively. Sulfuric acid diffuses and attacks the amorphous cellulose chains to cause chain scissions into small soluble oligosaccharides and sugars, leaving crystalline CNCs. Sulfuric acid also causes surface esterification to yield acid half ester or cellulose sulfate on the CNC surfaces, resulting in negatively charged surfaces and providing the repulsive forces to prevent CNCs from aggregation in aqueous suspensions.

Aqueous cotton CNC suspension was quickly frozen in liquid nitrogen and freeze-dried. Re-dispersion of freeze-dried cotton CNCs in ethanol was observed under TEM to show nanorods, spheres and porous network forms (Fig. 2). These three different forms of cotton nanocrystals could not be separated by filtration or centrifugation and have not been reported by others. The nanorods are less than 10 nm wide and 200–400 nm long (Fig. 2a), the width being similar to the 7.3 nm reported for cotton [22]. Spheres of 10–100 nm in diameters are the most abundant form (Fig. 2b). The porous network structure consists of 100–300 nm range interconnecting pores and is less observed than the rods and spheres (Fig. 2c).

The presence of nanospheres and network structures are likely to be artifacts of the processes used. These nanospheres, appearing porous and hollow, may be from association short nanorods by hydrogen bonds. The sources of the network structures could be from freeze-drying of CNC suspension, ethanol dispersion, drying in TEM sample preparation or a combination of these. The causes of the spheres and network forms are being further investigated by direct observation CNCs from aqueous suspensions. It should be noted that products of sulfuric acid hydrolysis, even under a fixed condition, are expected to be heterogeneous in sizes and structures from any source. This is due to the varying diffusivities of the less ordered regions and varied crystalline domain sizes as well as different cellulose chain lengths. The processes devised to separate the products, sample preparation for characterization as well as thoroughness in observation can contribute to the extents reported. In the cases of CNCs from these three cellulose sources, this hydrolysis and isolation processes were identical. Cotton CNCs were freeze-dried and then ethanol dispersed, whereas rice straw and grape skin CNCs were

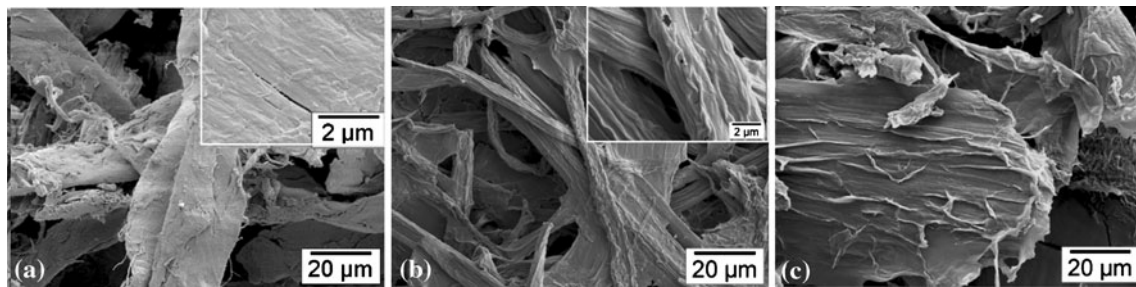


**Fig. 1** Pure cellulose from: **a** cotton; **b** rice straw; **c** Chardonnay grape skin

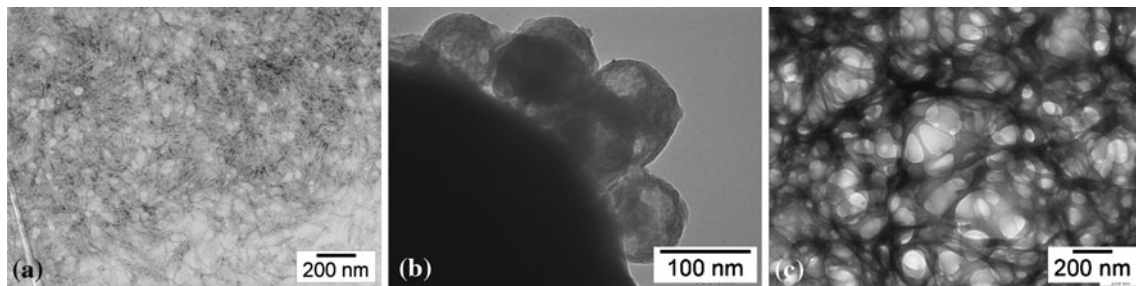


**Fig. 2** Cotton CNCs from freezing, freeze-drying and 0.005 % ethanol re-dispersion (TEM): **a** nanorods; **b** spheres; **c** porous network

air-dried from suspension. Therefore, the observed morphologies for cotton CNC are likely related to freeze-drying and ethanol dispersion employed in sample preparation. This is to be further studied.

Rice straw cellulose was hydrolyzed for 30 (CNC30) and 45 (CNC45) min into CNCs at 6.43 and 4.83 % yields, respectively. The dimensions of CNCs decrease with increasing length of hydrolysis, with CNC30 averaged 30.7 nm wide and 270 nm long, whereas CNC45 averaged 11.2 nm wide and 117 nm long as determined from 200 CNC images each from TEM, all with CV between 31 and 39 % (Fig. 3). The length-to-width or aspect ratios, on the other hand, slightly increase with longer hydrolysis time and are 8.8 and 10.5 for CNC30 and CNC45, respectively. The thickness of CNCs was determined by AFM height profiles to averages of 5.95 nm and 5.06 nm for CNC30 and CNC45, respectively, and, with 34 % CV for both, are not significantly different [18]. The much smaller thickness dimensions than their corresponding widths of 30.7 and 11.1 nm show both CNCs to be flat ribbon like, but at different width-to-thickness ratios of 5:1 and 2:1 for CNC30 and CNC45, respectively. The length/width/thickness ratios for CNC30 and CNC45 are 44:5:1 and 20:2:1, respectively, showing both CNC width and length reducing to less than one half with increasing hydrolysis time from 30 to 45 min. The similar thickness for CNC30 and CNC45 suggests size reduction in CNCs with increasing hydrolysis time to be mainly in the width and length.

Grape skin CNCs appear as spherical nanoparticles with diameters ranging from 10 to 100 nm diameters and mostly between 30 and 65 nm (Fig. 4a). These grape skin CNCs have a  $48.1 (\pm 14.6)$  nm mean diameter calculated from 169 CNC images. The phase images of AFM also show predominantly nanospheres (Fig. 4b) with occasional observation of nanorods (Fig. 4c). The heights of these nanospheres were all below 5 nm (height scale on right of Fig. 4b). Intriguingly, AFM images reveal the presence of few rods in the center of the larger spheres as well as many much smaller nanoparticles. The rods are mostly less than 100 nm in lengths, whereas the small nanoparticles are less than 5 nm in sizes. Furthermore, the spherical dimensions shown in the AFM are two to three times larger than those observed in TEM. These nanospheres retain their spherical shapes when captured on the hydrophobic carbon TEM grids. Even with the tip broadening effect expected in AFM, these much larger latter dimensions coupled with the 5 nm thickness suggest these nanospheres to be clusters of smaller nanoparticles and rods that collapse, upon deposition onto the hydrophilic mica surface, to expose their nanorod cores and nanoparticle shells. These AFM and TEM images suggest that grape skin CNCs dried into mainly nanoparticles that contain averagely 50–100-nm-long nanorod cores surrounded with numerous less than 5 nm diameter fragments.

Under the same sulfuric acid hydrolysis conditions, CNCs derived from cotton, rice straw and grape skin cellulose generally consist of nanorods, but to very different

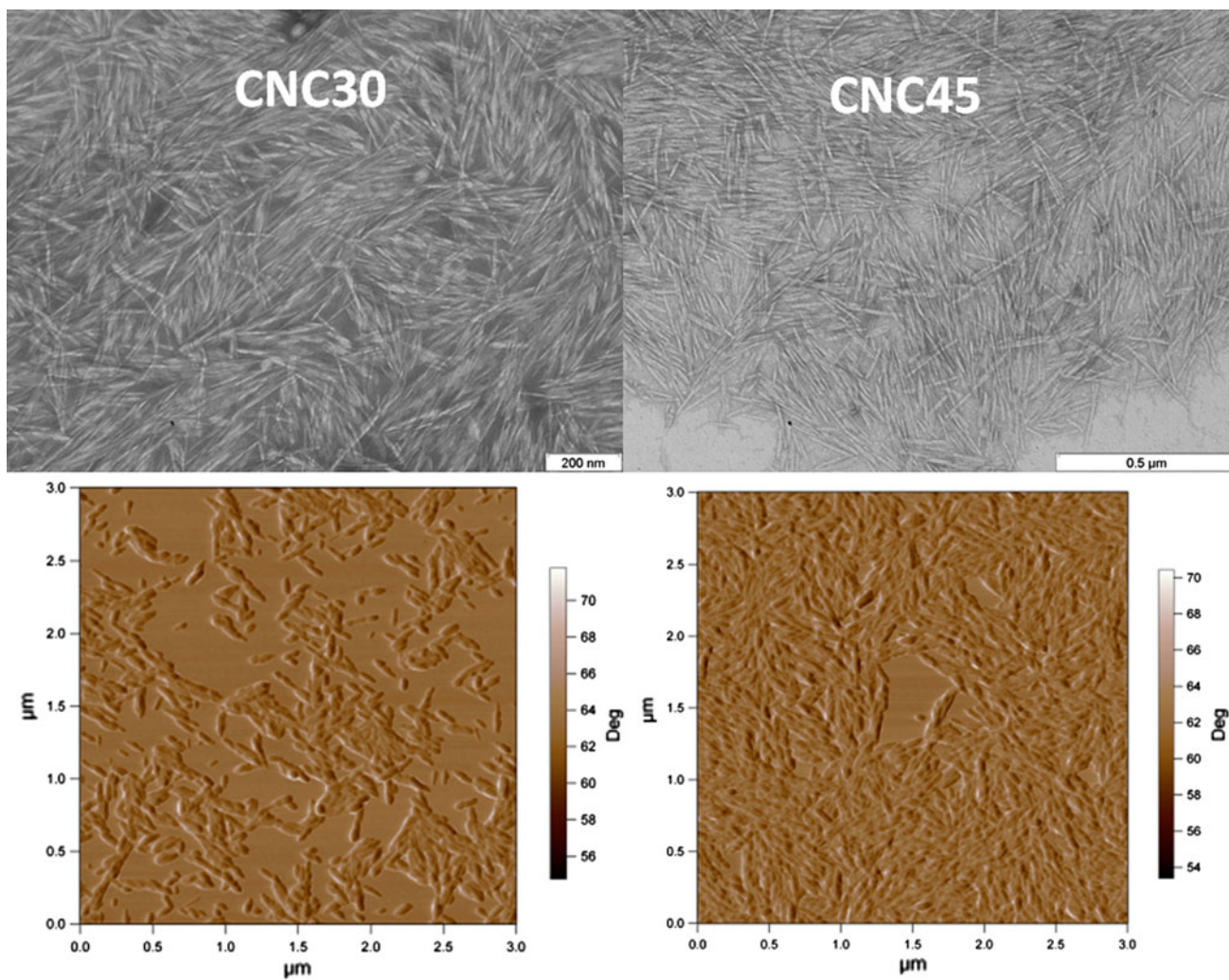


**Fig. 3** Rice straw CNCs: TEM (*top*) and AFM phase images (*bottom*). Samples were prepared from CNC concentrations of 0.005 % for TEM and 0.001 % for AFM

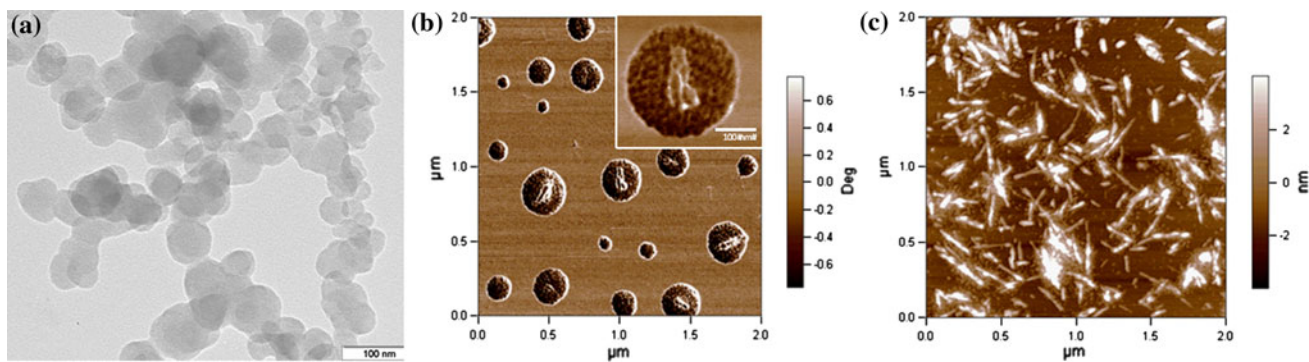


**Fig. 4** Grape skin CNCs (freeze-dried from 0.01 wt%): **a** TEM (0.001 wt%), **b** AFM (0.001 wt%) phase image of spheres, **c** AFM phase image of nanorods

extends and, in the cases of cotton and grape skin, also contain spherical forms (Table 1). The longest 60 min hydrolysis time necessary to derive consistent nanorods from cotton is consistent with the notion that cotton

cellulose molecular chain lengths are the longest as well as more ordered and crystalline. On the other hand, CNCs from grape skins were observed in the form of nanospheres and nanofragments mostly and, to a much lesser degree,

**Table 1** Geometries and dimensions of cotton, rice straw and Chardonnay grape skin CNCs

Cellulose source	Hydrolysis time (min)	CNC geometry	CNC yield (%)	CNC width (TEM)/ thickness (AFM) (nm)	CNC length (nm)	L:W aspect ratio
Cotton	60	Nanorods	NA	<10	200–400	20–40
Rice straw	30	Nanorods	6.43	30.7 wide/5.95 thick	270	8.8
	45	Nanorods	4.83	11.2 wide/5.06 thick	117	10.5
Grape skin	30	Nanorods	NA	<10 wide	50–100	5–10
		Nanoparticles		<5 wide	NA	NA

nanorods, suggesting the grape skin cellulose to be less crystalline and possibly less fibrillar. Rice straw CNCs derived from different hydrolysis times are similar in thickness that are also in the similar range as widths reported for wood pulp (4.3 nm) [22, 23]. The widths and lengths of rice CNCs, dependent of length of hydrolysis time as expected, are very different than CNCs from other sources. The length/width aspect ratios of nanorods are similar for cotton (20–40) and rice straw (20–44) CNCs, whereas the length/thickness ratios of rice straw (8.8–10.5) and grape skin (5–10) CNCs are similar, but lower.

Nanorod-shaped CNCs have been most commonly reported from sulfuric acid hydrolysis of wood and other sources as observed here with cotton and rice straw. CNCs generated from sulfuric acid hydrolysis of grape skin cellulose, on the other hand, are mainly spherical with nanorods occasionally observed. Cellulose in native plant cells has been commonly assumed to be in hierarchical fibrillar structures that are imbedded between hemicellulose and lignin. It is known that cotton cellulose has much longer chain lengths and also much more crystalline than cellulose in wood and other plants. Cellulose in the secondary cell wall of cotton is also 100 % pure cellulose. Spherical cellulose nanoparticles are much less observed and have been reported by hydrolysis of microcrystalline and pulp cellulose with a mixture of sulfuric and hydrochloric acid [24, 25] and, with NaOH and DMF pretreatment, producing cellulose II structure [25]. While the exact sources of nanoparticles or mechanism of nanosphere formation observed on cotton and grape skin CNCs are being further investigated, some thoughts are offered as follows. Both the chemical isolation and acid hydrolysis processes could possibly cause fragmentation of the cellulose into smaller and different shapes that deviate from the nanofibrillar forms. Furthermore, either the isolation or hydrolysis chemical processes as well as the preparation of samples for imaging and characterization could possibly cause fragmentation and/or association of the nanocellulose. Except for the different cellulose isolation processes between rice straw and grape skin, all other hydrolysis and sample preparation processes are identical. These

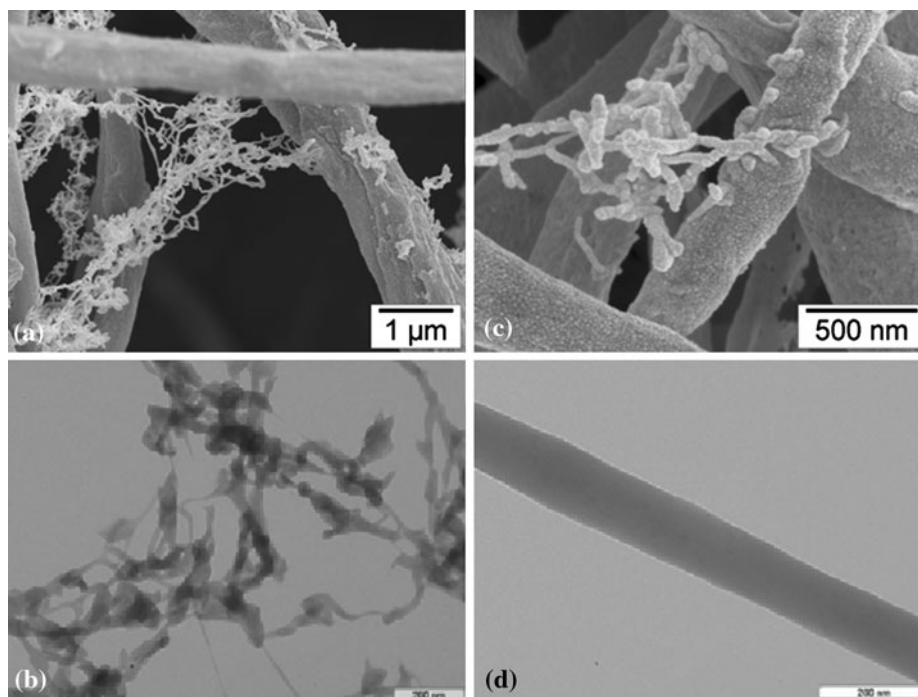
distinctively different geometries and dimensions of cotton, rice straw and grape skin CNCs clearly affirm a strong link to the sources that likely reflect their ultrastructure in the specific plants and cellulose crystallite dimensions. Such distinction could be exploited for building new materials from these uniquely structured nanocellulose building blocks.

#### Freezing and freeze-drying

The dilute aqueous CNC suspensions were frozen by liquid nitrogen ( $-196\text{ }^{\circ}\text{C}$ ) and then freeze-dried ( $-50\text{ }^{\circ}\text{C}$ ) into fluffy mass. As presented earlier, the freeze-dried cotton CNC is observed in three forms of nanorods, nanospheres and porous network (Fig. 2). Nitrogen gas adsorption further shows the freeze-dried cotton CNC to be mesoporous ( $91.99 \pm 2.57\text{ \AA}$  average pore width), showing no evidence micropores observed in the original pure cotton cellulose, and has significantly improved specific surface ( $13.362\text{ m}^2/\text{g}$ ) that is nearly nine times of the original cellulose ( $1.547\text{ m}^2/\text{g}$ ) [6]. These specific surface and pore sizes are consistent with the characteristics of nanospheres that are in the majority of the freeze-dried cotton CNC. The microporous nature of the original cotton cellulose is consistent with inter-molecular spaces among the amorphous chains which are removed upon hydrolysis, whereas the mesoporous nature of the freeze-dried structure reflects those of the inter-CNC pores. The freeze-dried cotton CNCs were easily dispersed into water, ethanol, DMF and other solvents in a matter of seconds without sonication. This easily dispersive behavior in a wide range of common solvents is highly desirable for versatile processing and making many potential applications possible. Therefore, the mesoporous structure of the freeze-dried cotton CNC is new and desirable characteristics.

From liquid nitrogen freezing and freeze-drying, rice straw CNCs self-assemble into long fibrous structures: broad 1–2- $\mu\text{m}$ -wide ribbons interspersed with CNC clusters (Fig. 5a) and strings of CNC from CNC30 (Fig. 5b) and ultra-fine fibers ( $\sim 400\text{ nm}$  wide) from CNC45 with very few CNC clusters (Fig. 5c, d). Furthermore, the self-

**Fig. 5** SEM (a, b) and TEM (c, d) of self-assembled rice straw CNCs



assembled ultra-fine fibers remained intact as observed under optical microscopy following vigorous shaking by hand and prolong mechanical stirring (300 rpm, 10 h), showing extraordinary structural stability. These assembled fibers could, however, be re-dispersed into aqueous CNC suspensions by sonication and reassembled under the same rapid freezing and freeze-drying conditions. Both the ability to self-assemble into fibers and that to be re-dispersed are unique and desirable characteristics of rice straw CNCs for versatile processing and applications.

Freeze-dried CNCs from grape skins were mostly observed in the forms of nanospheres and nanofragments, to lesser degree, nanorods as shown earlier (Fig. 4). During drying, the more abundant nanofragments associate around the fewer, but larger nanorods by strong hydrogen bonds and with each other, possibly driven by a layer-by-layer and thermodynamically favored process to the reduced specific surface. The assembled spherical nanoparticles have a  $48.1 (\pm 14.6)$  nm mean diameter, consisting of 50–100-nm-long rods surrounded by numerous <5 nm nanoparticles.

Freezing at  $-196$  °C followed by freeze-drying at  $-50$  °C of all three CNC suspensions leads to more crystalline assemblies of very different morphologies, i.e., mesoporous assemblies of rods and spheres from cotton CNCs [supplemental material b], non-porous or macroporous fibers from rice straw CNCs and nanospheres of nanorods surrounded by nanofragments (Table 2). These differently assembled structure from freeze-drying may be due to their very different CNC dimensions, i.e., much

higher aspect ratio for cotton CNC, the flat ribbon cross-sectional shapes of the rice straw CNCs and generally smaller nanorods and nanofragments of grape skin CNCs. Additionally, cotton CNCs have higher sulfur content (0.85 at.%) than rice straw CNC30 (0.18 at.%) and CNC45 (0.05 at.%), respectively [6, 18]. The lower surface charge nature of rice straw CNCs may explain the more compactly assembled fibers than those observed on cotton CNCs.

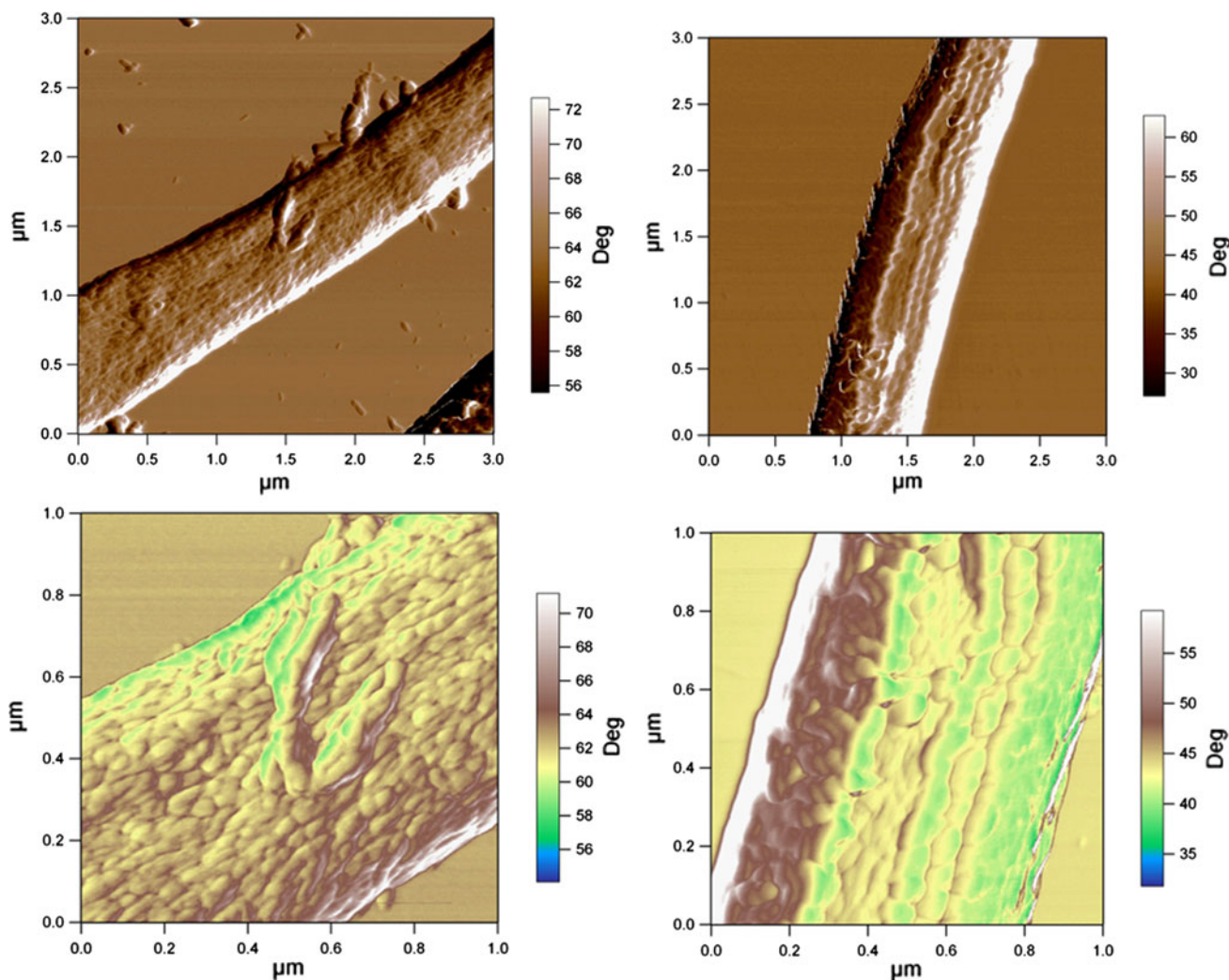
All freeze-dried CNCs from cotton, rice straw and grape skin show four XRD diffraction peaks at  $2\theta = 14.7, 16.4\text{--}16.6, 22.7$  and  $34.4^\circ\text{--}34.6^\circ$ , characteristic of cellulose I $\beta$  crystal assignments of the  $1\bar{1}0, 110, 200$  and  $004$  planes, respectively [supplemental material a]. The FTIR of all CNCs exhibited OH stretching at  $3270\text{ cm}^{-1}$  and OH out-of-plane bending at  $710\text{ cm}^{-1}$ , both characteristic of crystalline I $\beta$  structure [6, 18, 19]. The CrI value for grape skin CNCs is 64.3 %, less crystalline than those from cotton and rice straw or wood. The self-assembled fibers were more highly crystalline (86.0 and 91.2 % for CNC30 and CNC45, respectively) and contained 1 crystallites that are nearly double in sizes (7.36 and 8.33 nm, respectively) than the original rice straw cellulose (61.8 %, 4.42 nm) [18].

The 5.95 and 5.06 nm thicknesses of rice straw CNC30 and CNC45 are essentially in the same range, whereas their widths (30.7 and 11.2 nm) are about seven and two times of the average 4.42 nm crystalline dimension, respectively. This implies that under the current sulfuric acid hydrolysis condition, CNC of rice straw crystalline dimension may be derived at a time slightly longer than 45 min. This may

**Table 2** Self-assembled CNCs from freezing ( $-196\text{ }^{\circ}\text{C}$ ) and freeze-drying ( $-50\text{ }^{\circ}\text{C}$ )

CNC sample	CNC conc. (wt%)	Assembled morphologies	Fiber width/sphere diameter	BET surface area ( $\text{m}^2/\text{g}$ )	OrigCrI (%)	CNC CrI (%)
Cotton CNC60	0.005	Nanorods Nanospheres Porous network	<10 nm 10–100 nm	14.771	65	NA
Rice straw CNC30	0.06	1–2- $\mu\text{m}$ -wide fibers CNC clusters and strings	<10 nm	8.92	61.8	86.0
Rice straw CNC45		Ca. 400-nm fibers	$10^2$ nm	27.63		91.2
Grape skin CNC30	0.01	Spheres	48 nm	NA	54.9	64.3

Grape skin CNCs were observed as nanospheres<sup>a</sup> consisting 5 nm fragments surrounding nanorods<sup>b</sup>

**Fig. 6** AFM phase images of self-assembled rice straw CNCs: *left*: CNC30; *right*: CNC45

lead to the most crystalline and possibly approaching 100 % CrI for CNC from rice straw.

AFM phase images of the self-assembled rice straw CNC ultra-fine fibers showed undulated surfaces and CNC well

aligned along the fiber axis (Fig. 6). The height profiling of fibers from CNC45 showed a peak fiber height of 412 nm, comparable to the average fiber diameter ( $386 \pm 125$  nm) calculated from the SEM images, confirming cylindrical

cross-sectional shape of the CNC45 self-assembled fibers. For both assembled fibers, non-porous or macroporous nature was indicated by their type II BET isotherms with nearly reversible loops [19]. These self-assembled fibers had essentially non-porous or macroporous structures with the CNCs well aligned along the fiber axis.

The self-assembled fibrils exhibit extraordinary structural integrity that is attributed to the tight association of the CNCs. The unique ability of rice straw CNCs to self-assemble into uniform non-porous ultra-fine fibers is intriguing. Such self-assembling behavior is attributed to a combination of small dimensions (length, width and aspect ratio), ribbon-like cross-sectional geometries, strong interfacial attraction and possibly crystallization. This unique self-assembling behavior of rice straw nanocellulose derived with other chemical and mechanical means is being further investigated.

## Conclusion

Pure cellulose from cotton, rice straw and grape skin has been hydrolyzed by sulfuric acid into cellulose nanocrystals (CNCs). Under the same hydrolysis condition (64–65 wt% H<sub>2</sub>SO<sub>4</sub>, 10 mL/g cellulose, 45 °C), the times taken to achieve relatively consistent CNC products were 60, 45 and 30 min for cotton, rice straw and grape skin cellulose, generally reflecting the extent of crystallinity and crystallite sizes of these cellulose sources. CNCs derived from cotton, rice straw and grape skin cellulose generally consisted of nanorods, but to very different extents and, in the cases of cotton and grape skin, also consist spherical nanostructures. Cotton CNCs are <10-nm-wide and 200–400-nm-long nanorods and have the highest aspect ratio of the three. Rice straw CNCs are mainly flat ribbon-like nanorods with 44:5:1 and 20:2:1 length/width/thickness ratios from the 30 and 45 min reactions, respectively. Grape skin CNCs consist mainly <5 nm nanoparticles and some 50–100-nm-long rods. The aspect ratios of nanorods are in descending order of 20–40 for cotton CNC, 8.8–10.5 for rice straw CNCs and 5–10 for grape skin CNCs. These distinctively different geometries and dimensions of cotton, rice straw and grape skin CNCs clearly affirm a strong link to the sources that likely associated with their ultrastructure in the specific plants and cellulose crystallite dimensions. Such distinction could be exploited for building new materials from these nanocellulose building blocks.

Freezing (−196 °C) and freeze-drying (−50 °C) induced different morphologies in CNCs from different sources and geometries, but all in cellulose I $\beta$  crystalline structure and are more highly crystalline than their original pure cellulose. Cotton CNCs assemble into mesoporous forms of loosely organized nanorods, nanospheres and

porous network that could be easily dispersed into water and common organic solvents for versatile processing into hybrids and nanocomposites. Rice straw CNC self-assembled highly oriented, non-porous ultra-fine fibers that are unique to rice straw cellulose and is not observed with cotton nor grape skin CNCs nor reported on CNCs from other sources. These fibers are structural stable under vigorous shaking and prolonged mechanical stirring, but could also be re-dispersed into aqueous suspensions by sonication for reassembling or other uses. Grape skin CNCs are mainly spherical clusters of nanofragments with larger ones showing nanorod cores.

The feedstock for CNCs is diverse, abundantly available and renewable. While CNCs have been studied and reported extensively mostly from wood and other fiber crops, much less is known about crop and processing by-products. These analyses and comparisons of CNC derived from the top three fiber, cereal and fruit crops in the world with the same sulfuric acid hydrolysis clearly show strong structural dependence on their sources. The source-linked structural uniqueness of CNCs and their ability to assemble from rapid freezing and freeze-drying into different morphologies demonstrate further potential of some of nature's most abundant nanobuilding blocks.

**Acknowledgements** The author appreciates the fine experimental work by Ping Lu and Feng Jiang and funding from the California Rice Research Board, the National Textile Center and US Department of Agriculture, National Institute of Food and Agriculture.

## References

- Saxena IM, Brown RM Jr (2005) *Ann Bot* 96(1):9. doi: [10.1093/aob/mci155](https://doi.org/10.1093/aob/mci155)
- Hanley SJ, Giasson J, Revol JF, Gray DG (1992) *Polymer* 33(21):4639. doi: [10.1016/0032-3861\(92\)90426-W](https://doi.org/10.1016/0032-3861(92)90426-W)
- Terech P, Chazeau L, Cavaille JY (1999) *Macromolecules* 32(6):1872. doi: [10.1021/ma9810621](https://doi.org/10.1021/ma9810621)
- Grunert M, Winter WT (2002) *J Polym Environ* 10(1/2):27. doi: [10.1023/A:1021065905986](https://doi.org/10.1023/A:1021065905986)
- Beck-Candanedo S, Roman M, Gray DG (2005) *Biomacromolecules* 6(2):1048. doi: [10.1021/bm049300p](https://doi.org/10.1021/bm049300p)
- Lu P, Hsieh Y-L (2010) *Carbohydr Polym* 82(1):329. doi: [10.1016/j.carbpol.2010.04.073](https://doi.org/10.1016/j.carbpol.2010.04.073)
- Samir MASA, Alloin F, Dufresne A (2005) *Biomacromolecules* 6(2):612. doi: [10.1021/bm0493685](https://doi.org/10.1021/bm0493685)
- Helbert W, Cavaille JY, Dufresne A (1996) *Polym Compos* 17(4):604. doi: [10.1002/pc.10650](https://doi.org/10.1002/pc.10650)
- Sakurada I, Nukushina Y, Ito T (1962) *J Polym Sci* 57(165):651. doi: [10.1002/pol.1962.1205716551](https://doi.org/10.1002/pol.1962.1205716551)
- Sturcova A, Davies GR, Eichhorn SJ (2005) *Biomacromolecules* 6(2):1055. doi: [10.1021/bm049291k](https://doi.org/10.1021/bm049291k)
- Wong EW, Sheehan PE, Lieber CM (1997) *Science* 277(5334):1971. doi: [10.1126/science.277.5334.1971](https://doi.org/10.1126/science.277.5334.1971)
- Yu M-F, Lourie O, Dyer MJ, Moloni K, Kelly TF, Ruoff RS (2000) *Science* 287(5453):637. doi: [10.1126/science.287.5453.637](https://doi.org/10.1126/science.287.5453.637)

13. Klemm D, Kramer F, Moritz S, Lindström Ankerfors TM, Gray D et al (2011) *Angew Chem Int Ed* 50:5438. doi: [10.1002/anie.201001273](https://doi.org/10.1002/anie.201001273)
14. Production Statistics, Food and Agriculture Organization of the United Nations, <http://faostat.fao.org>
15. Hsieh Y-L (2006) In: Gordon S, Hsieh Y-L (eds) *Cotton science and technology*. Woodhead Publishing Ltd, Cambridge
16. Karimi K, Kheradmandinia S, Taherzadeh MJ (2006) *Biomass Bioenergy* 30(3):247. doi: [10.1016/j.biombioe.2005.11.015](https://doi.org/10.1016/j.biombioe.2005.11.015)
17. Spigno G, Pizzorno T, De Faveri DM (2008) *Bioresour Technol* 99(10):4329. doi: [10.1016/j.biortech.2007.08.044](https://doi.org/10.1016/j.biortech.2007.08.044)
18. Prozil SO, Evtuguin DV, Lopes LPC (2012) *Ind Crops Prod* 35(1):178. doi: [10.1016/j.indcrop.2011.06.035](https://doi.org/10.1016/j.indcrop.2011.06.035)
19. Lu P, Hsieh Y-L (2012) *Carbohydr Polym* 87(1):564. doi: [10.1016/j.carbpol.2011.08.022](https://doi.org/10.1016/j.carbpol.2011.08.022)
20. Lu P, Hsieh Y-L (2012) *Carbohydr Polym* 87(4):2546. doi: [10.1016/j.carbpol.2011.11.023](https://doi.org/10.1016/j.carbpol.2011.11.023)
21. Elazzouzi-Hafraoui S, Nishiyama Y, Putaux JL, Heux L, Dubreuil F, Rochas C (2008) *Biomacromolecules* 9(1):57. doi: [10.1021/bm700769p](https://doi.org/10.1021/bm700769p)
22. Jiang F, Esker AR, Roman M (2010) *Langmuir* 26(23):17919. doi: [10.1021/la1028405](https://doi.org/10.1021/la1028405)
23. Lahiji RR, Xu X, Reifenberger R, Raman A, Rudie A, Moon RJ (2010) *Langmuir* 26(6):4480. doi: [10.1021/la903111j](https://doi.org/10.1021/la903111j)
24. Cheng RS, Wang N, Ding E (2008) *Langmuir* 24(1):5. doi: [10.1021/la702923w](https://doi.org/10.1021/la702923w)
25. Ragauskas AJ, Zhang JG, Elder TJ, Pu YQ (2007) *Carbohydr Polym* 69(3):607. doi: [10.1016/j.carbpol.2007.01.019](https://doi.org/10.1016/j.carbpol.2007.01.019)